Natalia Konieczna

Comprehensive Procedure of the Assessment of the Quality of Welded Joints Made in Alloy INCONEL 617

Abstract: The development of the power engineering industry forces designers and material engineers to develop and implement new technologically advanced materials, including alloy Inconel 617. There are numerous works concerning tests focused on the alloy microstructure, yet welded joints made of Inconel 617 have not been discussed in detail. The description of the microstructure of welded joints provides designers, design engineers and welding engineers with knowledge enabling them to assess the service life and degradation of welded joints in elements made of Inconel 617. The article presents the analysis and the assessment of the microstructure of TIG-welded joints made of nickel alloy Inconel 617. The tests involved the use of light and scanning microscopy. Precipitates revealed in the tests were identified using EDS-based chemical composition microanalysis XRD-based phase analysis. The verification of the test results also required the performance of analysis carried out using the scanning transmission electron microscope. The tests revealed the presence of precipitates both in the base material and in the weld. The presence of precipitates including $Cr(Mo)_{23}C_6$ or Ti(CN) carbides increases the strength of the alloy, whereas identified dislocations and twins intensify the hardening effect.

Keywords: welded joints, microstructure, Inconel 617, nickel alloys, testing methodology

DOI: *10.17729/ebis.2018.6/4*

Introduction

Nickel-based alloys constitute a group of technologically advanced materials, the use of which is justified only in cases of the most aggressive operating conditions. For this reason, nickel alloys have found applications primarily in the aviation and power engineering industries, where operating temperatures exceed 650°C. Favourable mechanical properties of alloys exposed to high temperatures, such as creep strength, brittle crack resistance, resistance to thermo-mechanical loads, corrosion resistance, resistance to oxidation and structural stability determine their use in the fabrication of, among other things, aircraft engine elements such as rotor disks, compressor housings and high-pressure turbine blades. In the power generation industry, nickel alloys are primarily used in the production of crucial boiler elements, e.g. steam superheater coils and chambers [1,2].

mgr inż. Natalia Konieczna (MSc Eng.) – Silesian University of Technology, Institute of Materials Engineering, Katowice

Nickel alloys vary as regards their chemical composition and hardening type (related to applied heat treatment). Unlike in the aviation industry, the power engineering sector utilises solid solution hardened nickel alloys. One of the above-named alloys is Inconel 617, referred to in design-related documentation as a material used to make crucial boiler elements exposed to a temperature of as many as 720°C (Fig. 1) [3].

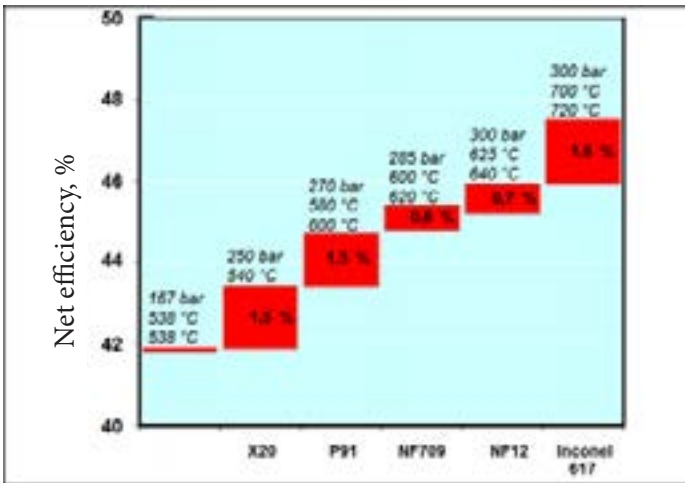

Fig. 1. Dependence of the net efficiency of the 400-700 MW power unit on the material and thermodynamic parameters of steam in pressure elements [3]

The need for reducing the emission of pollutants into the atmosphere necessitates the development of materials. Power units exposed to advanced ultra super critical parameters (AUSC) (Advanced Ultra Super Critical) will be designed for operation at a temperature of 700/720°C. The foregoing will require the use of creep and heat resisting materials. Subjected to appropriate heat treatment, alloy Inconel 617 can be successfully used in the fabrication of crucial boiler elements [4, 5].

In spite of the fact that alloy Inconel 617 was developed and implemented in the 1970s, its applicability-related tests, performed by a German research group known as Cooretec, started as late as in 2002. The research activities involved R&D carried out within project FDBR02 and DE-4, the objective of which was to improve the effectiveness of power plants as well as the separation and transport of CO_2 [6]. Presently, research works are focused on the applicability of the above-named material in heat exchangers of nuclear reactors (programme US DOE) [7].

Inconel 617 belongs to the group of the Ni-Cr-Mo-Co type alloys. Molybdenum and cobalt provide the alloy with good mechanical properties, whereas chromium provides corrosion resistance and, combined with nickel, provides structural stability. The modified variant of the alloy named Inconel 617B has been provided with an addition of boron, increasing creep strength [1,8].

Related scientific publications contain information concerning the material and properties of the alloy. However, there are no detailed characteristics related to the microstructure of welded joints made of Inconel 617. The welding process is a technological operation commonly used in the power engineering industry. For this reason, the obtainment of knowledge concerning the effect of electric arc on the microstructure of welded joints made of Inconel 617 is of vital importance. Once possessed, the above-named information will undoubtedly extend knowledge concerning welded joints made of solid solution hardened nickel alloys and enable the evaluation of the service life of welded joints in power engineering equipment.

Test materials and methodology

Materials used in the tests were butt welded joints made in 3 mm thick sheets of alloy Inconel 617. The chemical composition of the alloy in the as-received state was verified using X-ray fluorescence (XRF) (Table 1). The test results revealed that the alloy satisfied the requirements of the ASME standard [9]. According to the conformity certificate, the heat treatment involved solutioning, i.e. annealing at a temperature of 1177°C followed by cooling with air for 144 s. The sheets made of Inconel 617 were mounted in appropriate fixtures enabling the stabilisation of welding arc. The joints were made manually using the TIG welding

method. The welding process was shielded by argon fed at a flow rate of 10 l/min. The filler metal (2.4 mm in dimeter), the chemical composition of which is presented in Table 2, was similar to the base material. Welding parameters presented in Table 3 were adjusted so that it would be possible to obtain full penetration. The welded joints were assessed in accordance with the PN EN ISO 17637 standard. The analysis revealed that the joint made using the higher linear energy (Table 3, Fig. 2a) represented quality level B according to PN EN ISO 5817. In turn, the joint made using the lower linear energy, containing a crack located in the weld, failed to satisfy the requirements of quality level D (Table. 3, Fig. 2b). The joints were sampled for test specimen. The test specimens were cut out of the joints perpendicularly in relation to the direction of welding. The analysis involved the three characteristic areas of the welded joint, i.e. the base material (BM), heat affected zone (HAZ) and the weld. The test specimens were included in thermosetting resin to enable the performance of observations using a scanning electron microscope (SEM). In order to obtain appropriate metallographic specimens, the test specimens were subjected to grinding and polishing involving the use of diamond slurries. To reveal their microstructure, the metallographic specimens were subjected to electrochemical etching in Lucas' reagent. The 20-second long etching process was performed using a voltage of 6 V.

The tests included the analysis of the macro and microstructure of the welded joints using an Olympus SZX stereoscopic microscope (SM) and the dark field observation technique. The analysis at a magnification of up to 500x was performed using an Olympus SX71 light microscope and the bright field observation technique. The analysis of precipitates in the structure performed at a magnification exceeding 500x involved the use of an S 3400N scanning electron microscope (SEM) and the EDS-based microanalysis of the chemical composition. The tests were extended by the XRD-based phase analysis of precipitates. The precipitates were verified using a Hitachi S2300A scanning transmission electron microscope (STEM). The substructure was assessed using the above-named technique and a magnification of up to do 100000x.

Test results

The analysis of the cross-section of the joint made at a welding rate of 1.38 mm/s revealed the proper geometry of the weld, the face of

Table 1. Chemical composition of nickel alloy INCONEL 617, % by weigh [9]

IN617	Cr	Co	Mo	Al	Fe	Mn	Si	Ti	Cu	S	P	B	C
XRF	19.17	12.11	9.87	-	0.89	-	-	0.28	-	-	-	-	-
ASME SB-168:2013	20-24	10-15	8-10	0.8-1.5	max 3.0	max 1.0	max 1.0	max 0.6	max 0.5	max 0.015	-	max 0.006	0.05-0,15

Table 2. Chemical composition of the filler metal wire, % by weight [10]

ERNiCrCoMo-1													
Heat	C	Si	Mn	P	S	Al	Co	Cr	Cu	Fe	Mo	Ni	Ti
XX4751UK	0.084	0.03	0.05	0.004	0.001	1.16	11.60	22.50	0.02	1.00	9.10	54.00	0.34

Table 3. Parameters used in the welding of butt joints in 3 mm thick sheets made of alloy INCONEL 617

Current	Voltage	Welding rate	Welding linear energy
I, A	U, V	Vs, mm/s	EL, kJ/mm
80	25	1.38	0.870
90		2.27	0.595

which was characterised by smooth and even interface (Fig. 2a). The shape factor, defined as the weld width-weld height ratio amounted approximately to 1. An increased welding rate of 2.27 mm/s led to the formation of a hot crack located in the weld axis (Fig. 2b). The crack was formed at the beginning of the welding process. The analysis of the macrostructure in the crack area confirmed that the crack was hot and formed as a result of tensile stresses generated during crystallisation. The hot crack was characterised by bridges (Fig. 2b), i.e. areas of contact between crystal ends, distorted within the high-temperature brittleness range (ZKW).

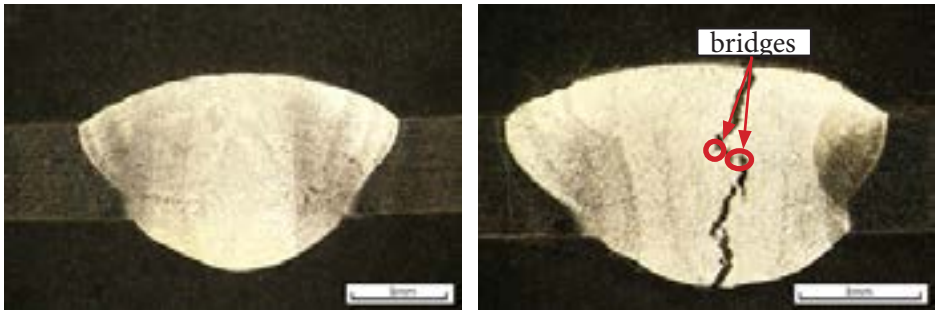

Fig. 2. Cross-section of the welded joints made in INCONEL 617 (SM):
a) at a linear energy of 0.87 kJ/mm, proper weld;
b) at a linear energy of 1.62 kJ/mm, the crack revealed in weld axis

The test results obtained using the light microscope (Fig. 3) confirmed information contained in reference publications [11,12], according to which alloy Inconel 617 was characterised by polygonal grains of the nickel-chromium matrix with precipitates both along the grain boundaries and within the grains (Fig. 3a). The structure contained alloy-hardening twins. In the heat affected zone, the weld crystallites accrued on the partially melted grains of matrix γ, forming the fusion line (Fig. 3b). The heat affected zone was typical of those exposed to the welding thermal cycle's effect. The observation did not reveal the presence of liquation cracks. The crystallites in the weld were elongated and accrued in accordance with the direction of heat discharge. (Fig. 3c). In addition, the observation revealed the presence of a hot crack along the crystallite boundaries (in the intercrystalline manner). The crack area contained distorted crystallites in the weld (Fig. 3d), indicating that the aforesaid area was exposed to a temperature restricted within the ductility-dip temperature range, i.e. a temperature, at which the plasticity of the structure occurs.

The SME-based analysis of the base material of Inconel 617 performed at a magnification of up to 3000x confirmed the presence of varying precipitates. The precipitates within the grains were globular, whereas those along boundaries were lamellar (Fig. 4a). In addition, the tests revealed a cluster of precipitates in the eutectic area (Fig. 4b) and involved the microanalysis of the chemical composition of the precipitates. The test

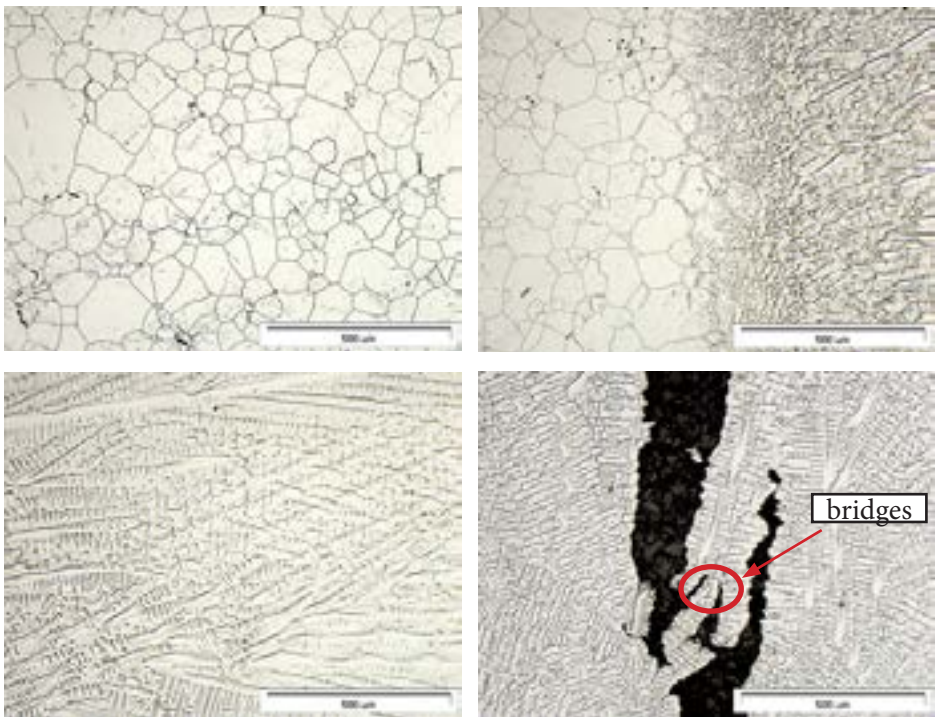

Fig. 3. Microstructure of the welded joints made in INCONEL 617, LM:
a) polygonal Ni-Cr matrix grains in the base material; b) accruing crystallites on the partially melted grains of matrix γ in the HAZ; c) elongated crystallites in the weld material; d) intercrystalline crack in the weld, E_L=1.62 kJ/mm

results are presented in Fig. 5. The tests revealed that the precipitates were primarily composed of molybdenum and chromium, probably forming the $M_{23}C_6$ type secondary carbides improving mechanical properties at higher temperatures. It was thus confirmed that the matrix consisted primarily of nickel, chromium, molybdenum and cobalt. The XRD-based phase identification of the sheets in the as-received state confirmed information contained in reference publications. The primary phase constituting the alloy matrix was phase γ, i.e. the solid solution of nickel (Fig. 6).

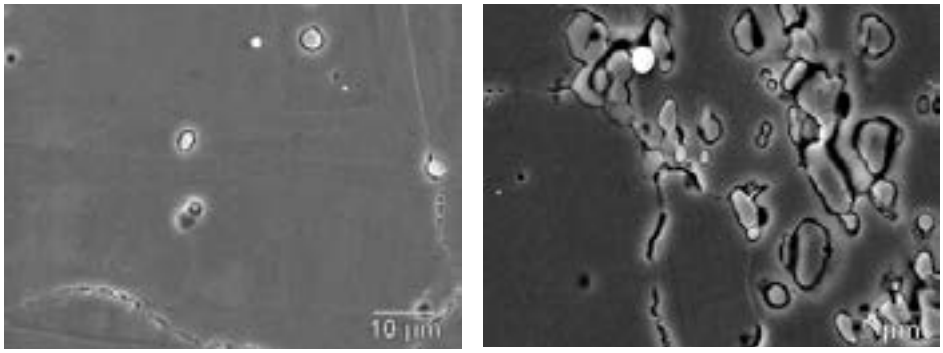

Fig. 4. Microstructure of the base material of INCONEL 617 (SEM): a) globular phase precipitates within grains and lamellar precipitates along the boundary; mag. 5000x, SE; b) complex precipitates in the eutectic area, mag. 10000x (BSE)

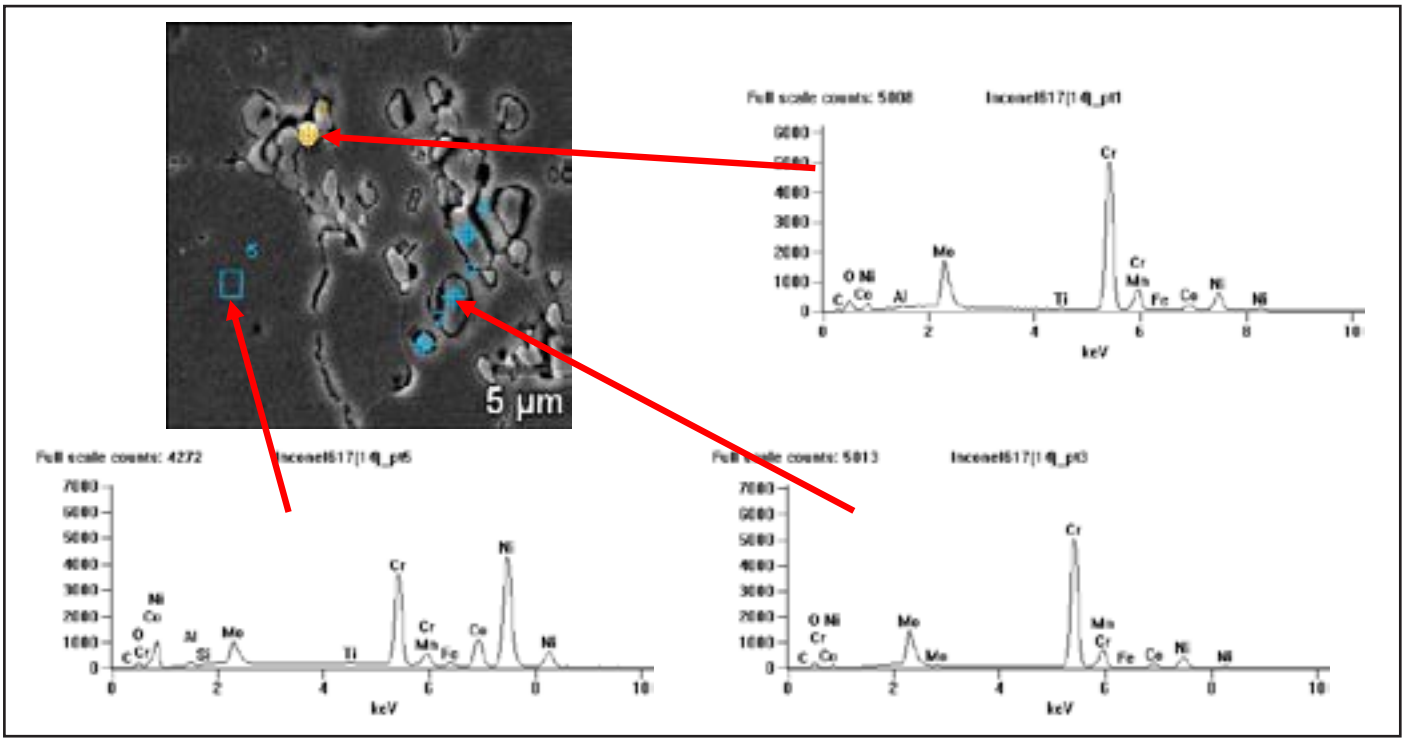

% at.	Al	Si	Ti	Cr	Mn	Fe	Co	Ni	Mo
pt1	0.3	-	0.1	58.9	0.1	0.4	4.2	12.4	23.5
pt2	0.4	-	0.2	51.3	0.1	0.7	5.6	22.8	19.1
pt3	-	-	-	65.1	0.1	0.4	3.2	9.6	21.6
pt4	0.1	-	0.2	58.9	0.1	0.3	3.9	10.6	25.9
pt5	1.1	0.1	0.3	23.0	0.1	0.7	11.6	11.6	9.1
% by weight	Al	Si	Ti	Cr	Mn	Fe	Co	Ni	Mo
pt1	0.7	-	0.2	67.2	0.1	0.4	4.2	12.6	14.5
pt2	0.8	-	0.2	58.1	0.1	0.7	5.6	22.9	11.7
pt3	-	-	-	73.5	0.1	0.4	3.2	9.6	13.2
pt4	0.2	-	0.2	68.1	0.1	0.3	4.0	10.8	16.2
pt5	2.4	0.3	0.4	25.8	0.2	0.7	11.4	53.4	5.5

Fig. 5. EDS-based microanalysis of the chemical composition of alloy INCONEL 617

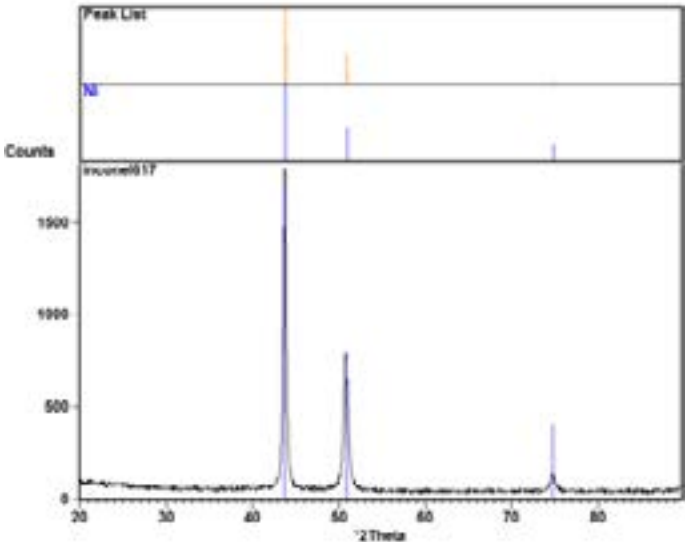

Fig. 6. Results of the phase analysis of alloy INCONEL 617

The tests were extended by observations involving the use of a scanning transmission electron microscope (Fig. 7). The extended tests included the EDS-based chemical composition analysis with results subjected to verification involving electron analysis. Magnifications of up to 1000000x revealed the dislocation structure in the base material of alloy INCONEL 617 (Fig. 7a). The detected dislocations were edge dislocations and, combined with a sufficiently high temperature, could lead to dislocation creep. In such a case, dislocations could obtain a new degree of freedom of movement, resulting in the ability to move (climb of edge dislocations). The observations also revealed the presence of twins (Fig. 7b). In the base material, subgrain boundaries were relatively free from phase precipitates. A different situation was observed in the weld, containing clusters of precipitates (Fig. 7c). The precipitates were globular, characteristic of $M_{23}C_6$. The substructure also revealed the presence of elongated carbides. Exemplary morphology is presented in Figure 7d.

The foregoing could be attributed to the effect of electric arc resulting in the melting of carbides followed by their spreading and solidification in the form of eutectics. The above-named process is discussed by the monograph by Professor E. Tasak [13] as the partial melting of carbides and belongs to reasons for hot cracking.

The substructural observations also revealed the presence of characteristically-shaped titanium carbonitrides (Fig. 8), which was confirmed by electron analysis. The electron analysis confirmed the presence of $M_{23}C_6$ (Fig. 9). The analysis of the surface distribution of individual chemical elements in the $M_{23}C_6$ carbide (Fig. 10) confirmed its composition including chromium and molybdenum. Nickel and cobalt were present in the matrix.

Summary

The test results revealed that the excessively high welding rate used when making joints in INCONEL 617 led to the formation of hot cracks. The crack appeared at a welding rate of 2.27 mm/s. In turn, the linear energy was lower than in the case of the first joint and amounted to

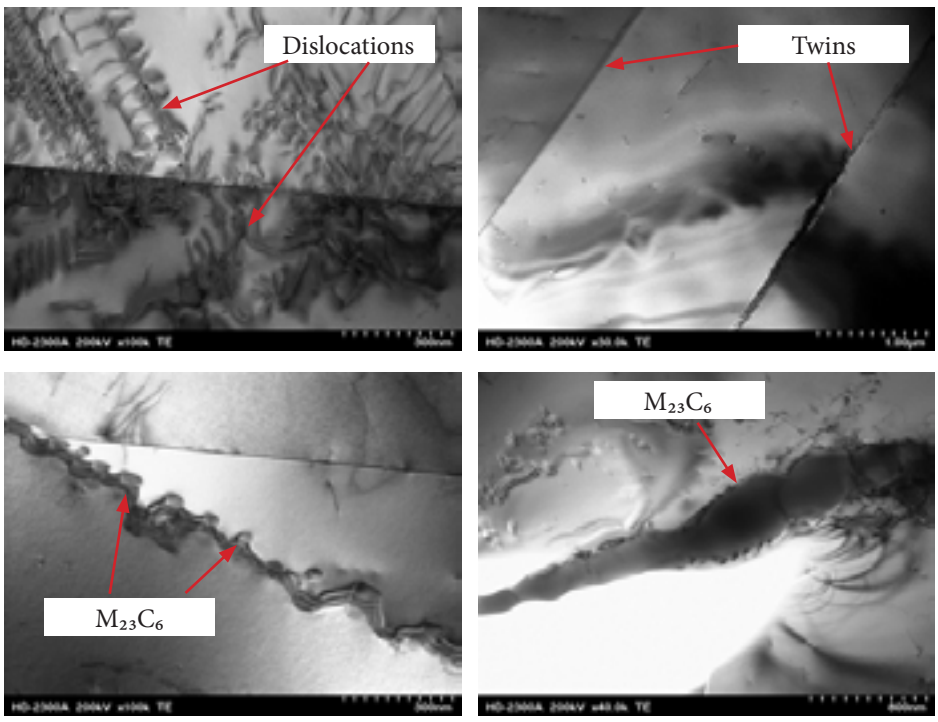

Fig. 7. Substructure of the welded joint made in INCONEL 617, STEM: a) subgrain boundaries in the base material; b) twins present in the alloy structure; c) subgrain boundaries with precipitates in the weld; d) elongated carbides in the weld material

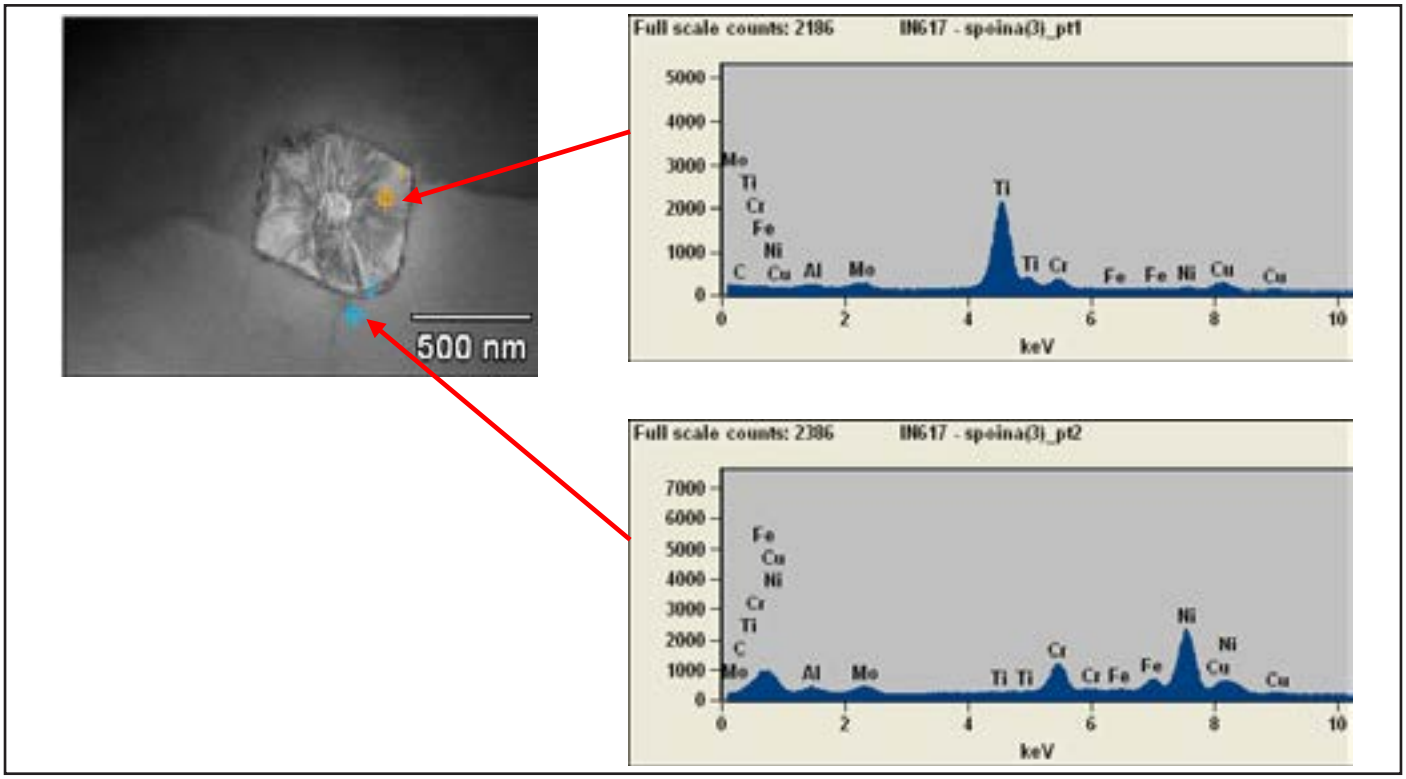

% at.	Al-K	Ti-K	Cr-K	Fe-K	Ni-K	Mo-L
IN617 - weld(3)_pt1	2.7	81.3	9.2	1.1	1.9	3.9
IN617 - weld(3)_pt2	7.8	0.0	24.3	6.3	54.9	6.7
% by weight	Al-K	Ti-K	Cr-K	Fe-K	Ni-K	Mo-L
IN617 - weld(3)_pt1	1.4	78.1	9.6	1.2	2.2	7.5
IN617 – weld(3)_pt2	3.7	0.0	22.2	6.2	56.7	11.3

Fig. 8. EDS-based microanalysis of the chemical composition (STEM)

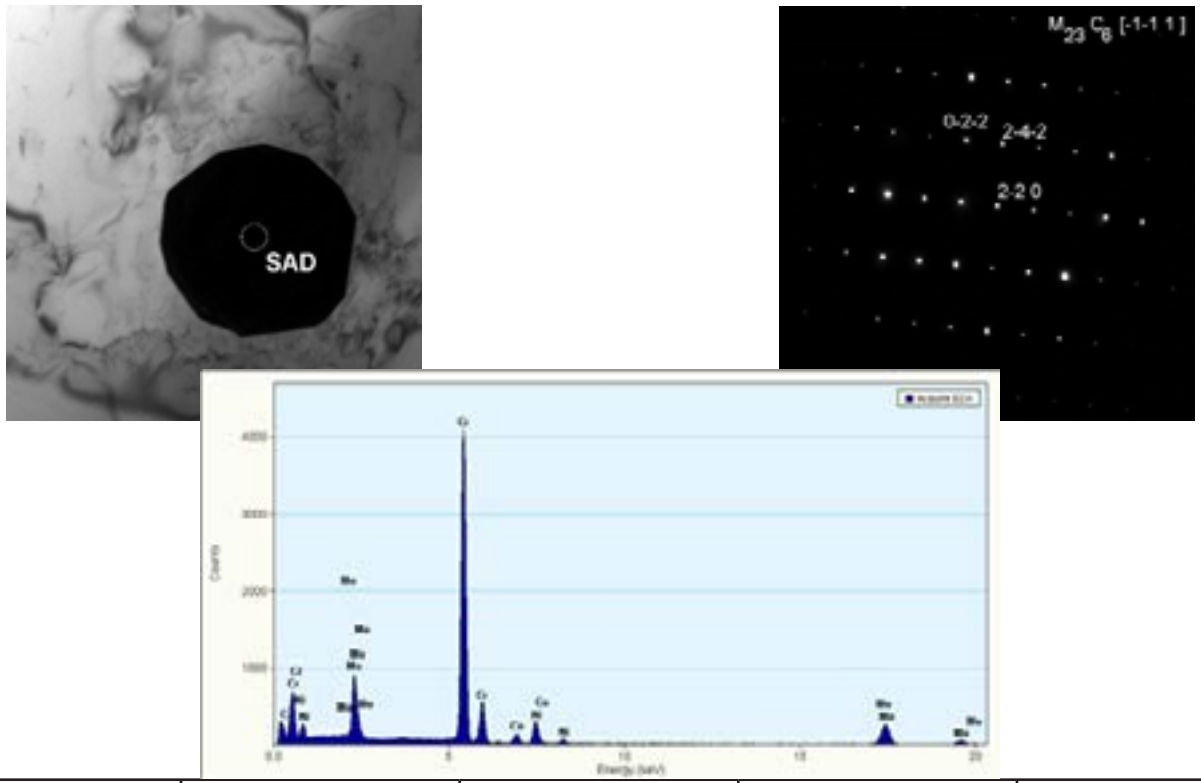

C	Cr	Co	Ni	Mo
6.58	62.88	2.56	5.34	22.64

Fig. 9. Electron analysis in the weld made in INCONEL 617

0.595 kJ/mm. To prevent hot cracks it is necessary to stabilise welding arc and maintain the welding rate not exceeding 2 mm/s. The above-named approach enables the obtainment of full penetration and, consequently, the lack of welding imperfections.

The base material of Inconel 617 was composed of polygonal grains of matrix γ with precipitates both along the grain boundaries and within grains. The heat affected zone was typical of that subjected to the welding thermal cycles. The observation did not reveal the presence of liquation cracks. The crystallites in the weld were elongated and crystallised in accordance with the direction of heat discharge. The precipitates present both in the weld and in the base material were composed of chromium and molybdenum and constituted $M_{23}C_6$ type secondary carbides. The presence of carbides precipitates was confirmed by electron analysis. The observations also revealed the presence of titanium nitrides within grains. Similar to carbides, titanium nitrides favour the obtainment of good mechanical properties. It was noticed that the carbides in the weld changed their morphology and were elongated. This could be ascribed to the partial melting of carbides and the formation of eutectics. The boundaries in the weld were composed of numerous carbide precipitates, providing high strength to the creep of the alloy. The structural constituents revealed during the observations consisted of dislocations and twins, hardening the alloy in operating conditions up to $0.4T_T$ of the alloy (T_T – melting point).

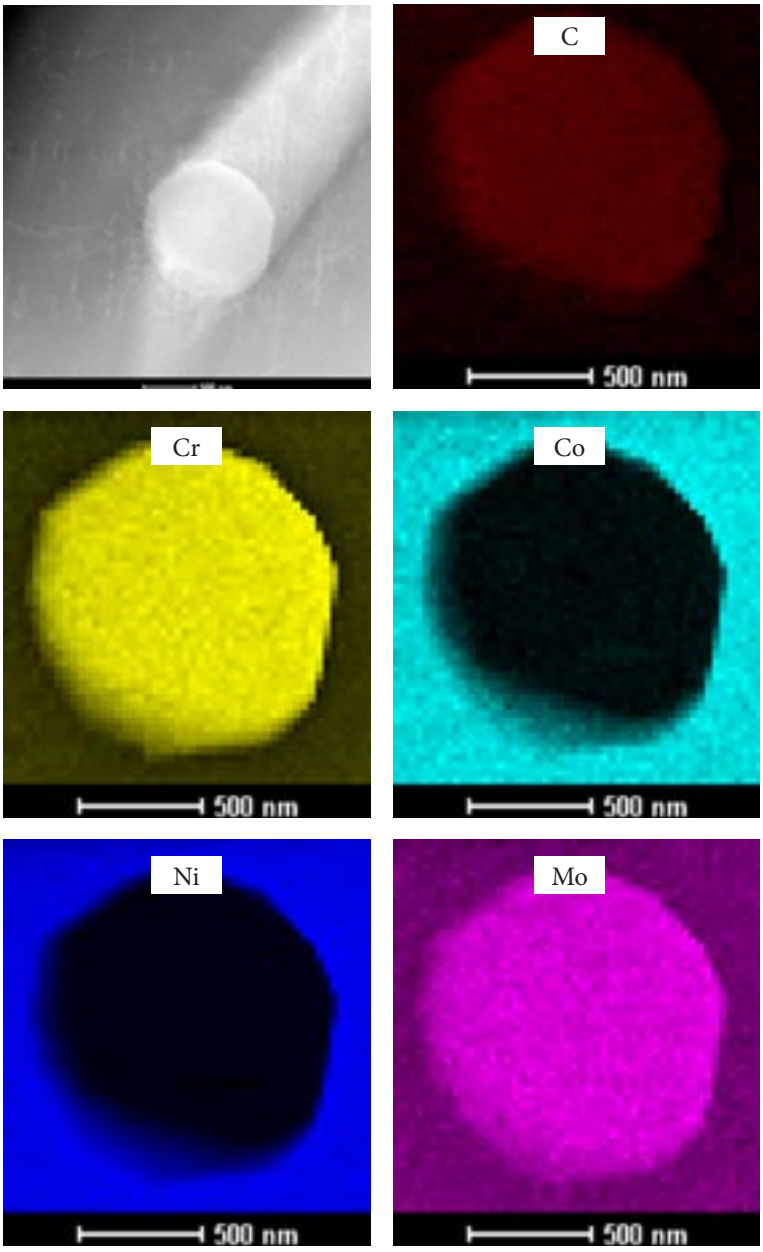

Fig. 10. Surface distribution of chemical elements in $M_{23}C_6$

The tests made it possible to develop the detailed procedure enabling the description of the microstructure of welded joints made of Inconel 617. The first stage of the procedure involved the verification of the chemical composition based on a non-destructive method, i.e. X-Ray fluorescence (XRF). The above-named method was used to check the chemical composition of alloy Inconel 617 for its compatibility with ASME SB-168:2013. The macro and microstructure were assessed using metallographic specimens cut out perpendicularly in relation to the welding direction. Following a related recommendation, the structure of the joint made of Inconel 617 was revealed using electrochemical etching in Lucas' reagent. The subsequent stage involved the assessment of the quality of the weld face and that of the root. Related tests were performed in accordance with the PN EN ISO 17637 standard. The next stage included the evaluation of the welded joint macrostructure. The macroscopic tests were performed using

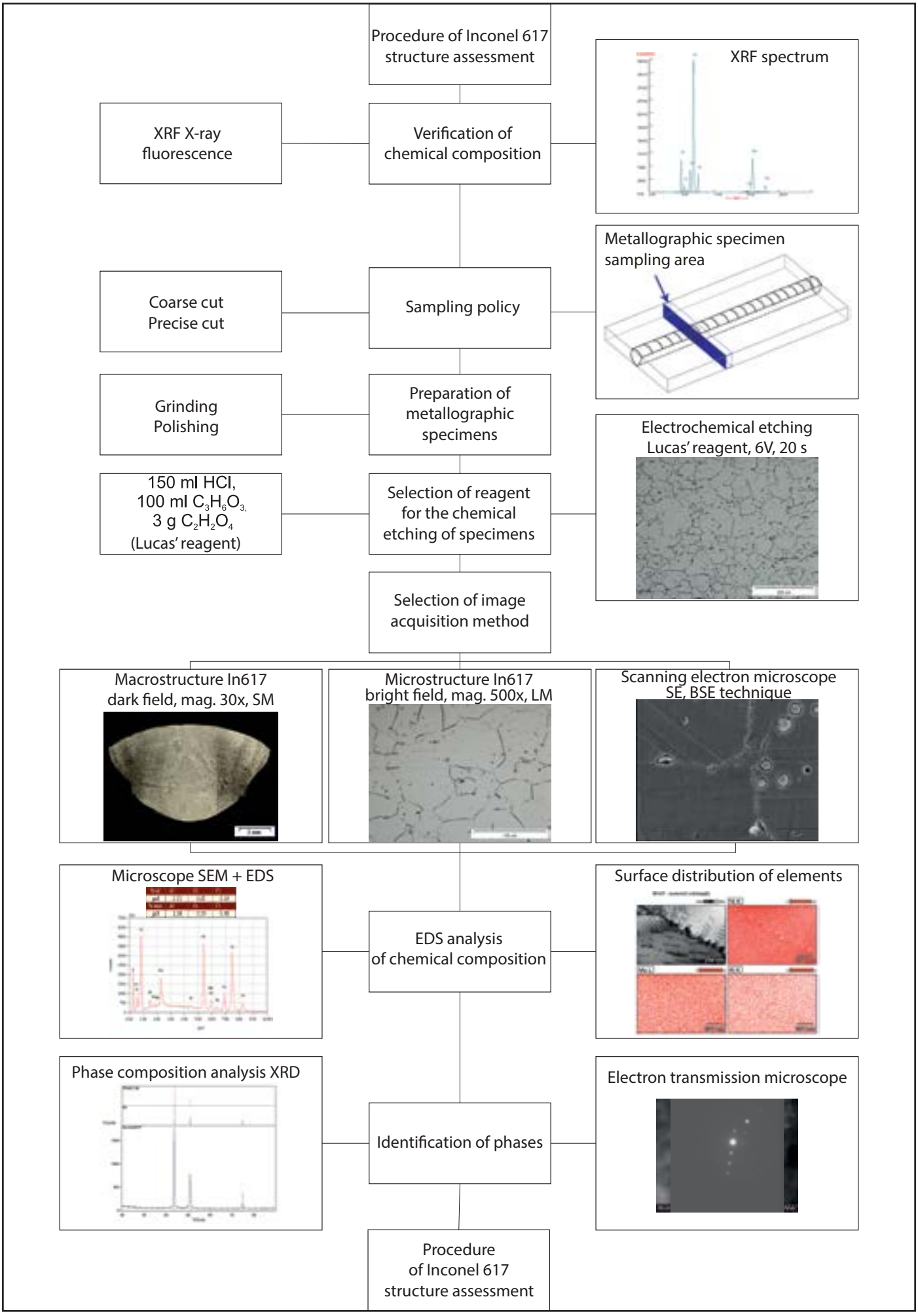

Fig. 11. Procedure of the assessment of the microstructure of the welded joints made in alloy INCONEL 617

a stereoscopic microscope and the dark field observation technique at a magnification of up to 50x. The microstructure of all of the zones of the joint was analysed using a light microscope and the bright field observation technique at a magnification of up to 500x. The tests were supplemented by observations performed using scanning electron microscopy (SEM) and the secondary electron (SE) as well as backscattered electron (BSE) technique at a magnification of up to 5000x. The material substructure was analysed using scanning transmission electron microscopy (STEM) at a magnification of more than 100000x. The chemical compositor of phases and precipitates present both in the material and in the joint were analysed using the microanalysis of the chemical compositor based on energy dispersive spectroscopy (EDS). The tests were performed using a scanning electron microscope (SEM) provided with an EDS-based chemical composition detector. The test results were then extended to include results obtained in the XRD-based analysis of chemical composition and results obtained in electron diffraction performed using a transmission electron microscope. The above-presented stage of the procedure enabled the identification of phases and constituents in the joint structure. The entire structure is presented schematically in Figure 11.

References

[1] Hernas A., Dobrzański J., Pasternak J., Fudali S.: Charakterystyki nowej generacji materiałów dla energetyki. Wydawnictwo Politechniki Śląskiej, Gliwice, 2015.

[2] Adamiec J.: Własności korozyjne napawanych warstw na elementach kotłów do spalania biomasy i odpadów komunalnych. W: Procesy niszczenia oraz powłoki ochronne stosowane w energetyce. 12-13 March 2015, Słok k/ Bechłatowa, pp. 201-218.

[3] Chmielewski A., Gumiński R., Mydłowski T., Radkowski S.: Wykorzystanie pary ultra nadkrytycznej w energetyce. Zeszyty Naukowe Instytutu Pojazdów, 2014, no. 2, pp. 45-51.

[4] Patel S. J., de Barbadillo J. J., Baker B. A., Gollihue R. D.: Nickel Base Superalloys for Next Generation Coal Fired AUSC Power Plants. Procedia Engineering, 2013, no. 55, pp. 246–252.

[5] Klöwer J., Husemann R. U., Bader M.: Development of Nickel Alloys Based on Alloy 617 for Components in 700°C Power Plants. Procedia Engineering, 2013, no. 55, pp. 226–331.

[6] Maile K.: Qualification of Ni-Based Alloys for Advanced Ultra Supercritical Plants. Procedia Engineering, 2013, no. 55, pp. 214–220.

[7] Ma L.: Identifying and Understandig Environment-Induced Crack Propagation Behavior in Solid Strengthened Ni-Based Superalloys. Project No. 09-803, 2012, University of Nevada.

[8] Li X., Kininmont D., Pierres R. L., Dewson S. J.: Alloy 617 for High Temperature Diffusion-Bonded Compact Heat Exchangers. Proceedings of ICAPP'08, Paper 8008, June 8–12, 2008.

[9] Norma ASME SB-168:2013: Specification for nickel-chromium-iron alloys (UNS N06600, N06601, N06603, N06690, N06693, N06025, and N06045) and nickel-chromium-cobalt-molybdenum alloy (UNS N06617) plate, sheet and strip.

[10] Certificate of the ERNiCrCoM-1 filler metal wire

[11] Stewart C.: Nickel–Based Super Alloys. INSG Insight. 2013, no. 20, pp. 1–9.

[12] Donachie M. J., Donachie S. J.: Superalloys: A technical Guide. Second Edition. ASM International. Printed in the United States of America, 2002.

[13] Tasak E.: Metalurgia spawania. Kraków, Wydawnictwo JAK, 2008.